PERGAMON

Deep-Sea Research II 49 (2002) 1173–1195

DEEP-SEA RESEARCH
PART II

www.elsevier.com/locate/dsr2

Winter and summer monsoon water mass, heat and freshwater transport changes in the Arabian Sea near 8°N

Lothar Stramma[a,*], Peter Brandt[a], Friedrich Schott[a], Detlef Quadfasel[b], Jürgen Fischer[a]

[a] *Institut für Meereskunde an der Universität Kiel, Düsternbrooker Weg 20, 24105 Kiel, Germany*
[b] *University of Copenhagen, Niels Bohr Institute, Juliane Maries Vej 30, 2100 Copenhagen, Denmark*

Abstract

The differences in the water mass distributions and transports in the Arabian Sea between the summer monsoon of August 1993 and the winter monsoon of January 1998 are investigated, based on two hydrographic sections along approximately 8°N. At the western end the sections were closed by a northward leg towards the African continent at about 55°E. In the central basin along 8°N the monsoon anomalies of the temperature and density below the surface-mixed layer were dominated by annual Rossby waves propagating westward across the Arabian Sea. In the northwestern part of the basin the annual Rossby waves have much smaller impact, and the density anomalies observed there were mostly associated with the Socotra Gyre. Salinity and oxygen differences along the section reflect local processes such as the spreading of water masses originating in the Bay of Bengal, northward transport of Indian Central Water, or slightly stronger southward spreading of Red Sea Water in August than in January. The anomalous wind conditions of 1997/98 influenced only the upper 50–100 m with warmer surface waters in January 1998, and Bay of Bengal Water covered the surface layer of the section in the eastern Arabian Sea. Estimates of the overturning circulation of the Arabian Sea were carried out despite the fact that many uncertainties are involved. For both cruises a vertical overturning cell of about 4–6 Sv was determined, with inflow below 2500 m and outflow between about 300 and 2500 m. In the upper 300–450 m a seasonally reversing shallow meridional overturning cell appears to exist in which the Ekman transport is balanced by a geostrophic transport. The heat flux across 8°N is dominated by the Ekman transport, yielding about –0.6 PW for August 1993, and 0.24 PW for January 1998. These values are comparable to climatological and model derived heat flux estimates. Freshwater fluxes across 8°N also were computed, yielding northward freshwater fluxes of 0.07 Sv in January 1998 and 0.43 Sv in August 1993. From climatological salinities the stronger freshwater flux in August was found to be caused by the seasonal change of salinity storage in the Arabian Sea north of 8°N. The near-surface circulation follows complex pathways, with generally cyclonic-circulation in January 1998 affected at the eastern side by the Laccadive High, and anticyclonic circulation in August 1993.

1. Introduction

The Arabian Sea undergoes large changes in response to the seasonal reversal of the monsoon winds, leading to a reversal of the Arabian Sea circulation and the Somali Current during the

*Corresponding author. Tel.: +49-431-600-4103; fax: +49-431-600-174101.
E-mail address: lstramma@ifm.uni-kiel.de (L. Stramma).

0967-0645/02/$ - see front matter
PII: S0967-0645(01)00169-2

different monsoon periods (Schott and McCreary, 2001). The climatological surface currents for the winter monsoon show the westward-flowing Northeast Monsoon Current (NMC, also called North Equatorial Current; Tomczak and Godfrey, 1994) south of India/Sri Lanka, which carries water from the Bay of Bengal toward the Arabian Sea. Along its way, some fraction of the NMC splits off northeastward toward the Indian coast, flowing anticyclonically around the Laccadive High with its center near 10°N, 70°E (Bruce et al., 1994). The NMC then continues westward at low latitudes toward the African coast, bifurcating off Somalia in the near-surface layer at about 8°N (Schott and Fischer, 2000). The southward-flowing branch of the upper-layer flow supplies the cross-equatorial Somali Current. The northward branch splits south of Socotra, with part of the flow continuing towards the Gulf of Aden through the passage between Socotra and the African continent (Fig. 1), while another fraction supplies the interior northern Arabian Sea around Socotra to the east (Schott and Fischer, 2000). The Ekman transport during the winter monsoon is northwestward in the interior Arabian Sea.

During the fully developed summer monsoon in August, the Somali Current is often characterized by a two-gyre system (Swallow and Fieux, 1982). During this period the Great Whirl north of 5°N is an almost closed anticyclonic circulation system and rather little exchange takes place with the interior Arabian Sea to the east. South of 5°N the anticyclonic Southern Gyre is developed in which the northward cross-equatorial Somali Current recirculates, with the offshore outflow partially flowing southward across the equator and partially feeding a low-latitude eastward flow.

South of India/Sri Lanka the Southwest Monsoon Current (SMC) is now developed, partially supplied from the west by the the Southern Gyre outflow. Off western India an upwelling regime exists during the summer monsoon, with southward surface flow and a northward subsurface undercurrent (Shetye et al., 1990). At its southern end there is a cyclonic circulation feature, the Laccadive Low (Shankar and Shetye, 1997). The Ekman transport in the interior Arabian Sea is southeastward during the summer monsoon. From sections along 8°30′N in the Arabian Sea Chereskin et al. (1997) computed a southward Ekman transport of 17.6 Sv for June 1995 and 7.9 Sv for September 1995. Air–sea flux calculations and model simulations suggest large seasonal changes of the meridional heat fluxes (Wacongne

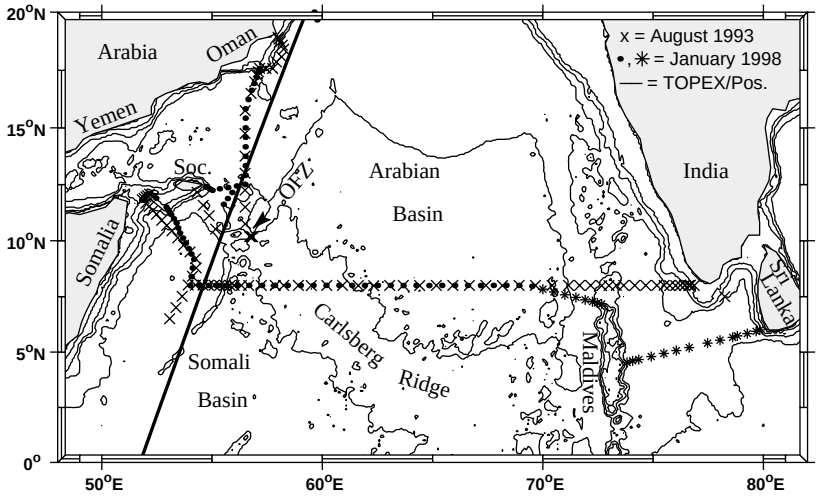

Fig. 1. CTD stations in the Arabian Sea from the cruises by R.V. *SONNE* during 5–25 August 1993 (cruise SO 89; crosses), 30 December 1997–4 January 1998 (cruise SO 127, stars) and 9–27 January 1998 (cruise SO 128, solid dots). Depth contours are shown for 200, 1000, 2000 and 4000 m. TOPEX/Poseidon path 233 is included as solid line. Soc. marks Socrota, OFZ shows the location of the Owen Fracture Zone.

and Pacanowski, 1996; Schott and McCreary, 2001). The important role of the Ekman transports was pointed out by Garternicht and Schott (1997) who found a high correlation between meridional heat transport and Ekman transport in an analysis of model fields.

In this study we use hydrographic parameter distributions, direct current measurements, and geostrophic velocity computations based on data sets from two R.V. *SONNE* cruises, in August 1993 (cruise SO 89) and January 1998 (cruise SO 128). The water mass and density differences and their causes will be investigated. The main objectives are the differences of the overturning circulations and heat transports in the Arabian Sea at 8°N during the southwest (summer) and northeast (winter) monsoon periods.

Several detailed studies using part of these data have been carried out previously. The August 1993 cruise was analyzed for the Great Whirl region (Fischer et al., 1996) and the flow field off southwest India at 8°N (Stramma et al., 1996), and the January 1998 cruise was evaluated for the winter circulation of the northern Somali Current region (Schott and Fischer, 2000). A companion paper of this issue focusses on the role of the annual Rossby waves along 8°N (Brandt et al., 2002). Here, the complete sections are analyzed and a comparison between the winter monsoon and the summer monsoon situation will be carried out. The in situ data collected during the cruises are supplemented by satellite-derived sea-surface heights.

2. Data and methods

Originally we had planned to occupy WOCE section IR1W line at 8°N. However, due to political constraints the ship had to stay out of the economic zone of Somalia and the sections at the western side were carried out northward and northwestward to the Somali–Socotra passage. In January 1998 (R.V. *SONNE* cruises SO 127 and SO 128) the ship also had to stay outside the economic zone of India. Two shorter sections from Sri Lanka to the central Maldives shelf and from the northern Maldives shelf to 8°N were made to close the IR1W section. The distribution of CTD stations during SO 89 in August 1993 and SO 127/SO 128 in January 1998 is shown in Fig. 1.

On all three cruises a narrow-band 150 kHz ADCP was used for underway current measurements. During August 1993 navigation data were supplied by a standard GPS and ship gyro, while in January 1998 the heading information by an Ashtech 3D-GPS and the major navigation source from a long range differential GPS improved the positioning and hence the accuracy of the current data. The current profiles were corrected for barotropic tidal constituents from model tides determined by Le Provost et al. (1998). We estimated the accuracy of the 1993 ADCP data to 10 cm/s for the raw 5-min data. As most of the errors arise from noise in the navigation and heading data, this error is reduced to about 5 cm/s in the 30-min averages. Less noise in the improved navigation data of January 1998 results in an error of about 2–3 cm/s for 30 min averages. The depth of the first reliable depth cell of the shipboard ADCP was 20–28 m, or a mean cell depth of 24 m. This is calculated from the transducer depth ($\sim$7 m), the blanking interval of 4 m and the omission of the uppermost depth cell that is contaminated by the flow around the ship and other error sources. Hence, large uncertainties occur in the upper 24 m of the water column, and the extrapolation (slab) towards the surface is only a crude estimate for the flow of the surface layer.

Hydrographic profiles were collected with a Neil-Brown Mark III CTD-system during the cruises SO 89 and SO 128 and a Seabird system during SO 127. The calibration of the CTD data resulted for all cruises in accuracies of 0.002°C in temperature, 0.003 in salinity, 4.5 dbar in pressure, and 0.07 ml/l for dissolved oxygen.

TOPEX/Poseidon altimeter data were processed for the period October 1992 to October 1998 for comparison with the northward ship section and for information on the temporal changes of some signals. Here we use the sea-surface height (SSH) anomalies from along-track data (Fu et al., 1994). To calculate regularly gridded SSH anomalies, the along-track data were interpolated by objective analysis to a $1^\circ \times 1^\circ$ grid with a temporal sample interval of about 10 days.

3. The water masses

3.1. The near-surface layer

The near-surface layer of the Arabian Sea near 8°N is influenced by three different water masses. The saline component is Arabian Sea Water (ASW) formed in the northern Arabian Sea during the northeast monsoon, when continental winds cool the ocean surface and strong evaporation causes the salinity to increase (Shetye et al., 1994; Morrison, 1997). The South Equatorial Current, the East African Coastal Current and the Somali Current during northern summer carry low-salinity water from the equatorial Indian Ocean into the Somali Basin (Swallow et al., 1983). Finally, the eastern side of the Arabian Sea off India receives low-salinity surface water from the Bay of Bengal (BBW) during winter.

3.2. The intermediate depth layers

The intermediate depth layers are occupied by three water masses. Warm and saline Persian Gulf Water spreads at 200–400 m depth, reaching latitudes of 5–10°N. Red Sea Water (RSW) is also characterised by high salinity and spreads at a core depth of about 500 m in the north and about 800 m at the equator. It can be traced as far south as the Agulhas Current (Beal et al., 2000a). The core layer densities of Persian Gulf and Red Sea Waters are $\sigma_\theta = 26.7$ and $\sigma_\theta = 27.25$, respectively. The third intermediate depth water mass originates in the south. Lower-salinity Indian Central Water (ICW), sometimes also called Subtropical Subsurface Water (Warren et al., 1966), originates at and north of the Subtropical Convergence in the southern hemisphere. It is characterised by an almost linear temperature–salinity relationship and enters the northern hemisphere via a western boundary current off the East African coast (Swallow et al., 1988). In the northern hemisphere this water mass is also referred to as Northern Indian Central Water (e.g. Gordon, 1986). A further characteristic of the Central Water is a weak oxygen maximum at a temperature of 11°C at around 400 m depth. Although the absolute oxygen content of this water mass is quite low, it is the major source of dissolved oxygen in the Arabian Sea. The central and northern parts of the Arabian Sea are known for their low-oxygen layer occurring in the depth range between 200 and 1200 m. The oxygen content everywhere north of 3°N is <1 ml/l (Wyrtki, 1973).

3.3. The deep water

The deep waters in the Arabian Sea, in contrast to the upper and intermediate layers, show much less spatial and temporal variability. Warren (1993) identified the layer between 1500 and 3500 m as North Indian Deep Water (NIDW). Below that layer Circumpolar Deep Water is found as bottom water. Bottom water enters the Arabian Sea through the Amirante Passage and flows northward along the western boundary of the Somali Basin (Johnson et al., 1991a). Some of it continues across the Carlsberg Ridge to form bottom water of the Arabian Basin (Johnson et al., 1991b). For the Owen Fracture Zone Quadfasel et al. (1997) estimated a transport of about 2 Sv below 3000 m depth from the Somali Basin to the Arabian Basin during the SW-monsoon 1995. Warren and Johnson (1992) described a broad south-westward flow in the deep-water layer of the eastern Arabian Basin during both monsoons. These patterns were not forced by the monsoons but reflected the mean circulation of the deep water as driven by upwelling of the bottom water from below. Because there is no other escape route from the deep Arabian Sea, the Bottom Water rises upward and is transformed into NIDW (Warren, 1993; Mantyla and Reid, 1995). The Deep Water acquires its characteristics here: high silica values by flux from the sediments and a higher salinity and lower oxygen content through vertical mixing with the much more extreme Intermediate waters above it. Evidence of enhanced vertical mixing in the northern Somali Basin has been discussed by Dengler (2000). He shows that buoyancy-scaled spectral energy of the internal wave field north of 7°N increases with depth, implying larger eddy diffusivities in the abyssal ocean.

4. Results

4.1. Ekman transports

The Ekman transport is the largest contribution to the meridional heat flux in the northern Indian Ocean (Garternicht and Schott, 1997). Chereskin et al. (1997) estimated the meridional Ekman transport across 8°N from the ageostrophic velocity component of the VMADCP at 17.6 ± 2.4 Sv (1 Sverdrup $= 10^6 m^3/s$) for June 1995 and 7.9 ± 2.7 Sv for September 1995. These direct estimates were in good agreement with those calculated from both shipboard and climatological winds. This good agreement also was found in slightly modified computations by Chereskin et al. (2002) for the zonally integrated sections, but with significant differences along parts of the sections.

Our own attempt to compute the Ekman transports from the difference between shipboard ADCP and geostrophy transports failed for our ship observations. For August 1993 the integrated 0–350 m shipboard transport was 25 Sv to the south. The geostrophic transport in this layer relative to 1210 dbar was 5.9 Sv, which combined with the −7.4 Sv Ekman transport from the scatterometer winds (see below) results in an imbalance of <2 Sv. The shipboard ADCP, however, leads to an imbalance of more than 16 Sv. Following Chereskin et al. (1997) by calculating the transports relative to a shallow 300 m reference did not improve the transport estimates based on the data from August 1993. The 0–300 m transports relative to 300 dbar are −22 Sv for the shipboard ADCP and 5.3 Sv for the geostrophic computations. Only a rather large systematic offset of 1.6 cm/s in the ADCP measurements that is integrated over the section length of 3000 km and a depth of 350 m would explain the large differences between the shipboard net section transport and the Ekman and geostrophic computations. However, absolute and relative transports are similar, with a difference of only 3 Sv suggesting that a bias should not be much larger than 0.5 cm/s. Instead, there are other more likely reasons that this method to estimate the Ekman transport does not work with our data set.

First, as explained before, the first realistic ADCP measurements are at 24 m depth. Using the equation for the Ekman surface velocity for Ekman's solution to the equation of motion with friction (e.g. Pond and Pickard, 1983) and an Ekman layer of 50 m with typical wind speed for August of 12 m/s on the western side of the 8°N section results in an Ekman surface velocity of 1.1 m/s. Wind speeds of 6 m/s are typical for the eastern side of the 8°N section in August and for wide parts of the section in January yielding an Ekman surface velocity of 0.3 m/s. The Ekman velocity decreases exponentially to 0 near 50 m depths and consequently a large fraction of Ekman transport takes place in the upper Ekman layer that is not resolved by the shipboard ADCP. Ekman transports estimated from the ERS-1 winds in August 1993 led to differences of 20% for linear extrapolation in the upper 24 m for an Ekman depth of 50 m and 10% for an Ekman depth of 100 m. Extrapolation to the surface therefore leads to an uncertainty of some Sv. More locally, but with large impact on the overall transport estimate, it was shown by Fischer et al. (1996) that the transports associated with the Great Whirl had large ageostrophic contributions from the curvature of the eddy circulation, which are measured by the ADCP but not by geostrophy. The scale factor arising from uncertainties in the sound speed estimate does not contribute to the error as it has been taken into account during the calibration process. A significant fraction of the ADCP transport is associated with the upper 25 m not contained in the geostrophic transports as the inspection shows. Errors from unresolved current features such as near-inertial currents are a dominant contribution to the uncertainties in the transports (Chereskin et al., 1997). We therefore conclude that the method to compute the Ekman transport as the difference between the ADCP transport and the geostrophic transport is less reliable when using our data set compared to calculating the Ekman transport directly from the wind observations. Therefore, we will not apply this approach for the flux calculations. Instead, our discussion is based on Ekman transports derived directly from wind observations. These are summarised in Table 1.

Table 1
Ekman transport computed for the 8°N section in the Arabian Sea, positive northward or towards the Arabian Sea, across 8°N but following the *SONNE* ship sections towards the north near the African shelf and in January 1998 also through the Maldives to Sri Lanka, which reduces the amount of Ekman transport compared to a straight 8°N section

Month	Ekman transport	Method
January 1998	3.3	Ship wind
January 1998	7.7 ± 3.0	ERS2
January 1998	6.8	FSU wind
January	5.5	HR wind
January	2.9	ECMWF-re.
August 1993	−4.9	Ship wind
August 1993	-7.4 ± 2.3	ERS1
August 1993	−8.3	FSU wind
August 1992	−11.4	FSU wind
August	−9.3	HR wind
August	−5.0	ECMWF-re.

HR indicates Hellerman and Rosenstein (1983) wind stress climatologies, ECMWF indicates reanalysed data set of monthly means of 5 typical years of the ECMWF (European Center for Medium-Range Weather Forecasts) wind data, FSU indicates monthly pseudo wind stress data from the Florida State University and ERS weekly satellite derived wind stress.

Ekman transports were calculated using three different synoptic data sets and two wind climatologies. Wind data were extracted along the respective ship tracks including the northward track in the western basin and may therefore differ from the fluxes across 8°N latitude. The comparability with Chereskin et al.'s (1997) estimates is thus limited. The lowest of the estimates based on the synoptic data is the one using the shipboard observations of R.V. *SONNE* (Table 1). Unfortunately, the wind sensors on R.V. *SONNE* were not well maintained and were located at unfavourable locations; a simple correction to the data could not be applied. The Ekman transports based on the satellite-derived weekly ERS1/2 scatterometer winds were about twice as high but close to the monthly FSU winds. The difference between the two does not exceed 1 Sv and is thus in the range of errors computed from the ERS wind errors provided with the ERS data set. The Hellerman and Rosenstein (1983) climatologies lead to a higher Ekman transport in August and to a lower value in January, which may be caused by unresolved year-to-year variability. It is believed that the Hellerman and Rosenstein winds are generally too high and have recently been used in a 20% reduced version (Qiu and Huang, 1995). Such a reduction would improve the August Ekman transport, but the January Ekman transport would deviate more from the other estimates of Table 1. The second climatology consists of monthly means of 5 years ECMWF-reanalysis data. These lead to the lowest Ekman transports for both months, but show fairly good agreement with the Ekman transports derived from the shipboard wind measurements. However, as the wind instruments on R.V. *SONNE* are known to be biased low, we use the ERS1/2 scatterometer weekly winds as the best estimate for Ekman transport of 7.7 Sv in January 1998 and −7.4 Sv in August 1993 (Table 1) across the cruise track.

For August 1993 Stramma et al. (1996) described that the wind off Sri Lanka and India were lower than normal. This is supported by the FSU data set in which the data from August 1992 were stronger than those of August 1993. Consequently, a weaker than normal Ekman transport is expected for August 1993. The time series of meridional Ekman transport across the Arabian Sea at 8°N from the ERS-scatterometer winds (Fig. 2) also indicate low Ekman transport in August 1993. The southward transport weakened earlier in 1993 leading to a weak positive anomaly in August 1993 (Fig. 2b). The summer monsoon during 1992 was generally stronger than during 1993. For the western tropical Indian Ocean Webster et al. (1999) and Yu and Rienecker (2000) described a deeper than normal thermocline and anomalous easterly surface winds in the equatorial region between 5°S and 5°N. The largest anomalies appeared between 60°E and 100°E for the winter 1997/98 leading to higher Ekman transport in January 1998. The meridional Ekman transport anomalies across 8°N showed large northward anomalies during the year 1997 (Fig. 2b). In January 1998 the Ekman transport across 8°N (Fig. 2) was larger than in January 1997 and the mean curve from all years. However, it is comparable to some of the earlier years, hence the Ekman transport anomaly described by Webster et al. (1999) for the equatorial region

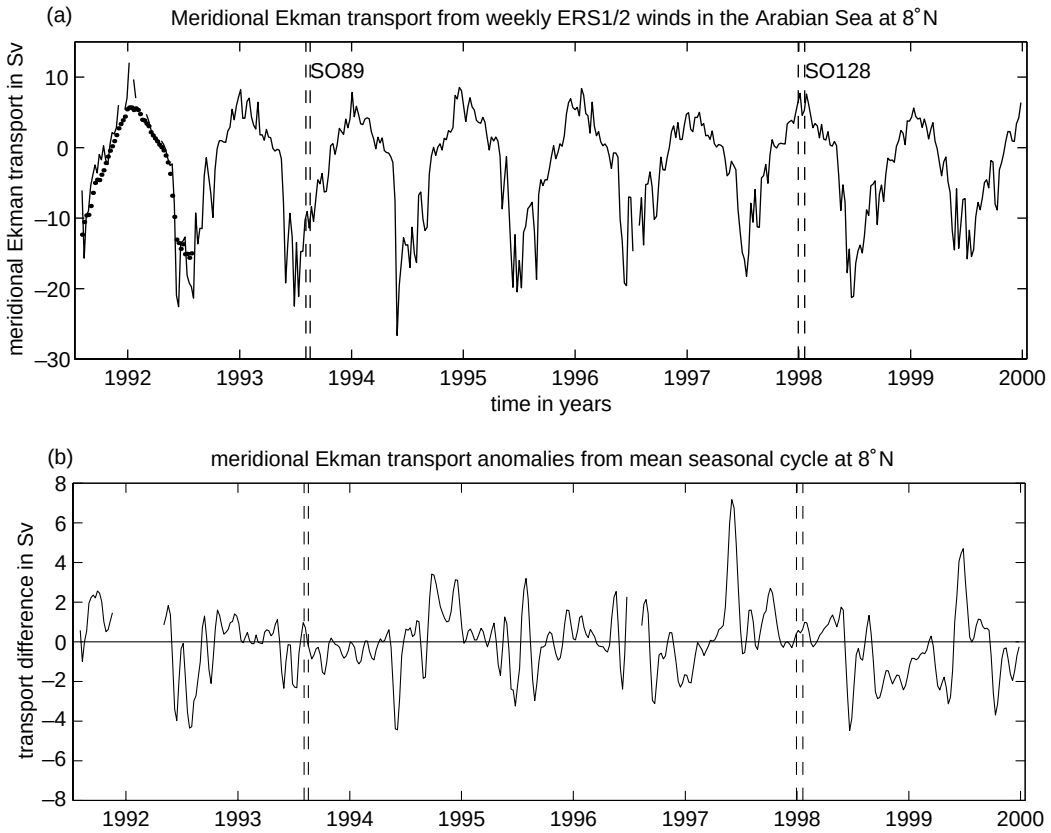

Fig. 2. Time series of meridional Ekman transport across 8°N in the Arabian Sea between 50.5°E and 79.5°E from (a) the ERS weekly wind fields (solid). The mean seasonal cycle of the meridional Ekman transport derived from all measurements is shown for the first year (dots). (b) The transport anomalies between the weekly wind fields and the mean seasonal cycle, smoothed by a running weighted average over 5 weeks. The time periods of the two cruises SO 89 in August 1993 and SO 128 in January 1998 are marked by dashed lines.

has only a small influence on the 8°N Ekman transport in January 1998. The *SONNE* cruise track in January 1998 was south of 8°N between Sri Lanka and the Maldives (Fig. 1). About half of the Ekman transport was contributed by the part between Sri Lanka and the Maldives (see Fig. 12b), hence the large Ekman transport in January 1998 along the cruise track was significantly influenced by the tropical 1997/98 anomaly between Sri Lanka and the Maldives.

4.2. Water mass and circulation changes

4.2.1. The zonal 8°N section

The distribution of water masses in the upper 1000 m along 8°N changes with the monsoons (Figs. 3–5). Below the layer close to the surface, the temperatures in August 1993 compared to January 1998 were higher on the western side of the Arabian Sea but lower on the eastern side. The largest differences are found around 100 m depth, reflecting a westward deepening and eastward shoaling of the thermocline. The temperature differences well represent the large-scale differences in density and can be related to annual Rossby waves propagating westward in the 6°N to 10°N band (Brandt et al., 2002). The salinity (Fig. 4) and oxygen distributions (Fig. 5) also show the effects of the tilting of the thermocline around 100 m depth but below 200 m the salinity differences are more scattered than those of temperature. The salinity and oxygen differences

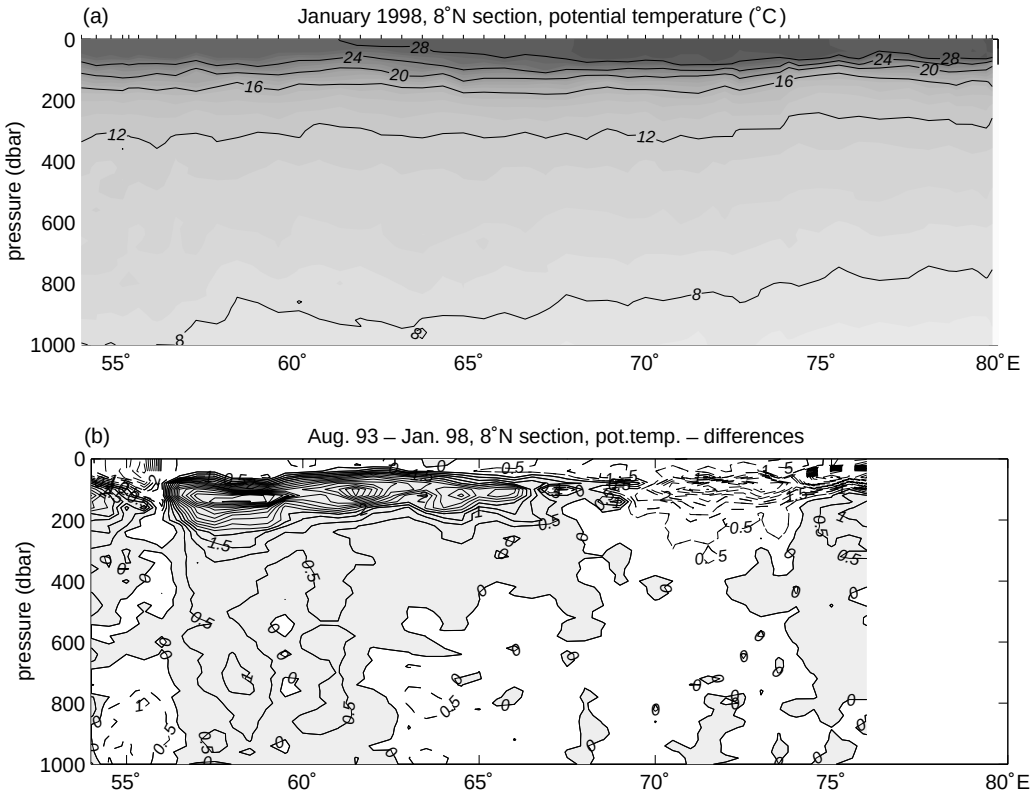

Fig. 3. (a) Potential-temperature distribution in °C of the upper 1000 m for the zonal section along about 8°N in January 1998 and (b) differences in potential temperature for August 1993 compared to January 1998 (positive differences represent higher potential temperatures in August 1993). Note that the January 1998 cruise track east of 70°E (see Fig. 1) is located south of 8°N but differences are computed comparing the longitudinal values.

probably reflect more local processes and mesoscale advection of water masses.

Webster et al. (1999) reported strong anomalies in sea-surface temperatures, sea-surface heights, precipitation and winds that occurred in the Indian Ocean region in the period 1997–98. An SST anomaly of more than 2°C was observed in the western Indian Ocean during February 1998. According to the climatological surface distribution (Levitus and Boyer, 1994a), the temperatures in January compared to August near 8°N should be higher near the African continent, at similar values in the central Arabian Sea and lower near India. In our specific comparison (Fig. 3) the upper 50–100 m are warmer in January 1998, representing the influence of the 1997–98 anomaly in the tropical Indian Ocean. However, this signal cannot be observed below the mixed layer.

In January 1998 low-salinity water from the Bay of Bengal was observed along the eastern side of the section at the sea surface above the saline Arabian Sea Water (Fig. 4a). During the winter monsoon the spreading of the BBW to the Arabian Sea is supported by the Ekman transport while during the summer monsoon the BBW is forced back to the south and east by the Ekman transport. However, some leakage of low-salinity water into the Arabian Sea may also occur during the SW monsoon. In July 1993 Schott et al. (1994) observed a narrow band of westward flow just south of Sri Lanka and in August 1993 Stramma et al. (1996) observed BBW also off the Indian coast at 8°N. This leakage in 1993 seemed to be

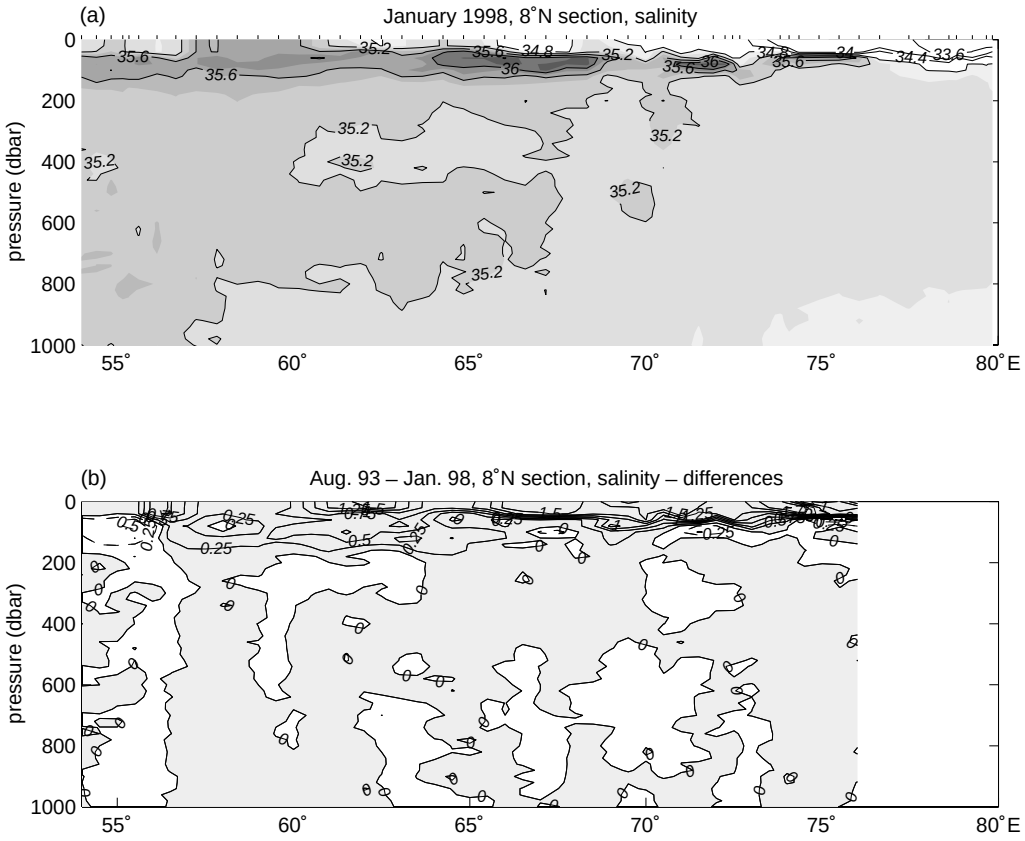

Fig. 4. Same as Fig. 3, but for salinity.

caused by lower than normal winds off India and Sri Lanka.

In August 1993 the ASW reached to the sea surface and salinities were enhanced. This is in agreement with the monthly distributions of ASW shown by Prasanna Kumar and Prasad (1999), where the southward spreading of ASW in August at 8°N was strongest in the central Arabian Sea. The less saline water in August 1993 at the western side of the section indicates a recirculation of SECW in the Great Whirl.

The low-oxygen layer between 150 and 1000 m depth in the central Arabian Sea contained slightly oxygen-richer water at 150–500 m depth (Fig. 5). The presence of this slightly oxygen-richer water leads to an oxygen minimum at about 150 m depth. The slightly oxygen-richer water was observed in large regions in January 1998 where the currents were northward (Fig. 6a) while in August 1993 the oxygen enhanced regions were restricted to the western side in regions of southward flow (Fig. 6b). As the increased oxygen values are related to slightly lower salinities, it shows that this was ICW flowing to the north in January 1998 and to the south in August 1993. The southward flow component in August can be explained by the fact that to the west of the 8°N section within the Somali economic zone the Great Whirl carried ICW northward and recirculated it within the western side of the August 1993 section.

Near the isopycnal of $\sigma_\theta = 27.25$ located at a depth of about 700 m the salinity distribution shows small maxima related to minima in oxygen distribution mainly on the western side of the 8°N sections of both cruises. This salinity maximum is difficult to detect in the section graph, but it is

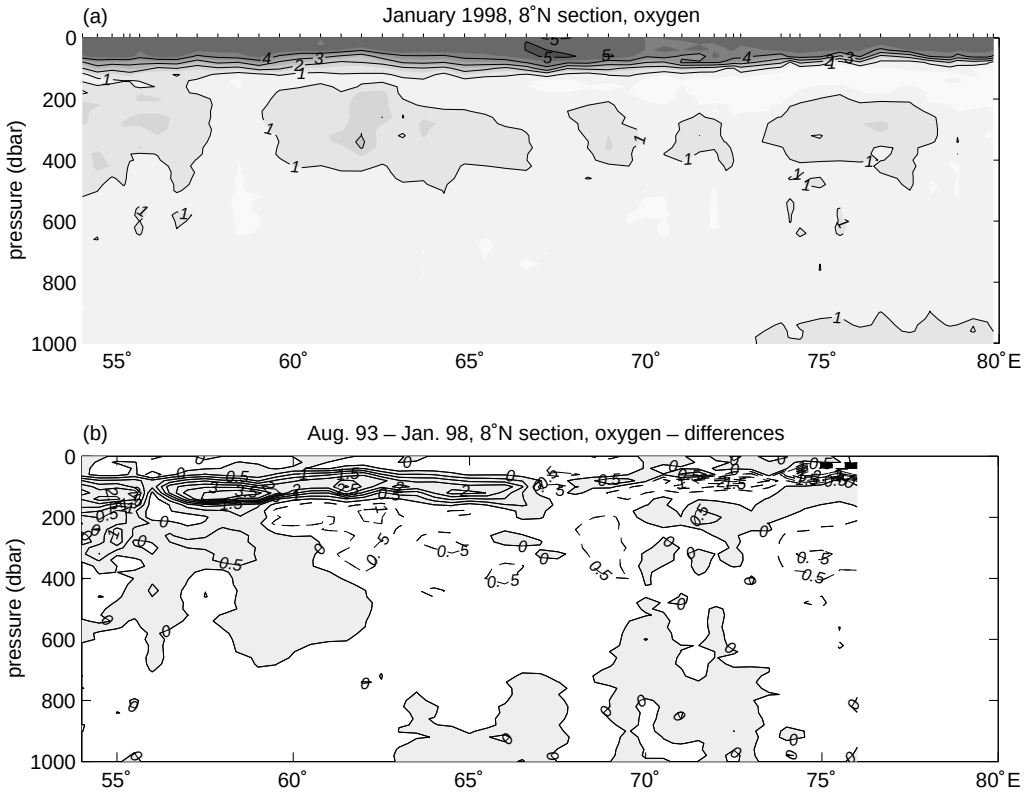

Fig. 5. Same as Fig. 3, but oxygen in ml/l.

obvious in the $T-S$ diagram (not shown here) and indicates the presence of RSW during both monsoon seasons although a little stronger in August 1993. It was observed at locations where the geostrophic velocity distribution indicates southward flow. No distinct salinity maximum at the isopycnal $\sigma_\theta = 26.7$ for PGW was observed at 8°N.

In the deep-water layer the differences between the two cruises decreased in magnitude. The density differences in the central Arabian Sea caused by the Rossby waves reverse sign in the deep ocean (Brandt et al., 2002) and so do the observed temperature differences, which are closely related to the density differences.

4.2.2. The northward 55°E section

The northward section (Fig. 7) is composed of the northwestward section from 8°N to the Socotra Passage and from there northward to the Arabian peninsula at about 56°30′E (see Fig. 1), with a zonal jump at 11°24′N. It is named 55°E section in the following. The differences between the seasons in temperature and salinity as well as oxygen are much more correlated here when compared to the 8°N section. Except for the very southern part, the 55°E section lies outside the region of the annual Rossby waves (Brandt et al., 2002) and local meso-scale processes and advection influence the parameter distribution and variability. In August the monsoon winds transport surface waters equatorwards. Upwelling appears near the Omani coast and the thermocline is shallow. In January water is transported northward by the Ekman transport and the upper ocean becomes warmer and saltier in the Arabian Sea (Prasanna Kumar and Prasad, 1999). The only region of higher temperatures in August 1993 in

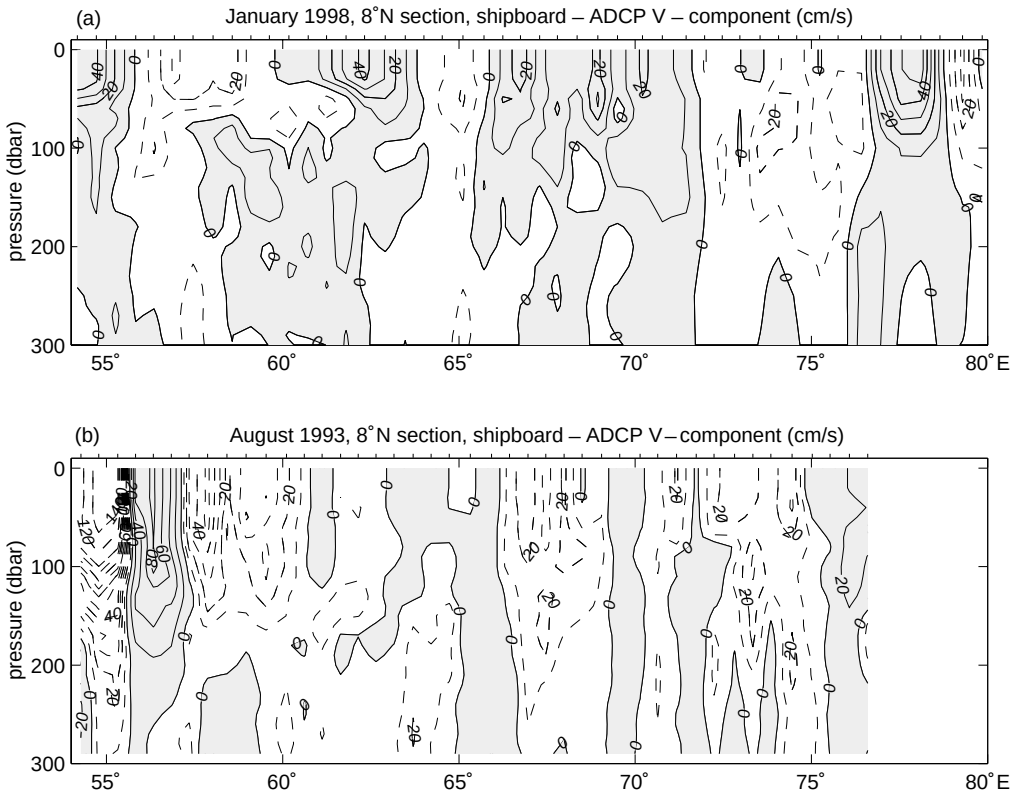

Fig. 6. Tidally corrected shipboard ADCP velocities along 8°N in cm/s for the upper 300 m of the sections in (a) January 1998 and (b) August 1993, positive is northward. The contour interval is 20 cm/s for velocities of more than 100 cm/s or else it is 10 cm/s. There may be a constant off-set of up to 3 cm/s. See text for details.

the upper 400 m north of 9°N is at 11°24′N to 13°N, where the Socotra Gyre carried warm and saline water eastward (Fischer et al., 1996).

Fig. 8a shows a Hovmoeller diagram of the SSH anomaly along TOPEX/Poseidon path 233 at about 55°E (see Fig. 1) for the period October 1992–October 1998. There is no indication of an annual Rossby wave north of about 10°N; hence this section mainly reveals local influences leading to the SSH elevation and depression. In this period the Socotra Gyre showed its strongest appearance during the summer monsoon of 1993 (Fig. 8a). The SSH anomaly differences and the integrated 0–1000 m density anomaly differences between August 1993 and January 1998 (Fig. 8b) show good agreement. The different geographical locations of the jump in sea-surface height anomaly differences between 11°N and 12°N are caused for the hydrographic section from the zonal jump of the section at 11°24′N and for the TOPEX/Poseidon data from the interpolation to a $1^\circ \times 1^\circ$ grid with values available only at 11°N and 12°N. Except for this location, the altimeter data reflect the local processes found in the difference of the two observed density distributions, with the largest signal caused by the Socotra Gyre.

4.3. Total transports, heat and freshwater fluxes

The sections along about 5°N east of the Maldives together with the 8°N section in January 1998 and along 8°N in August 1993 closed by the northwestward section toward the Socotra Passage close the Arabian Sea and allow calculations of the total overturning circulation, the heat and freshwater transport.

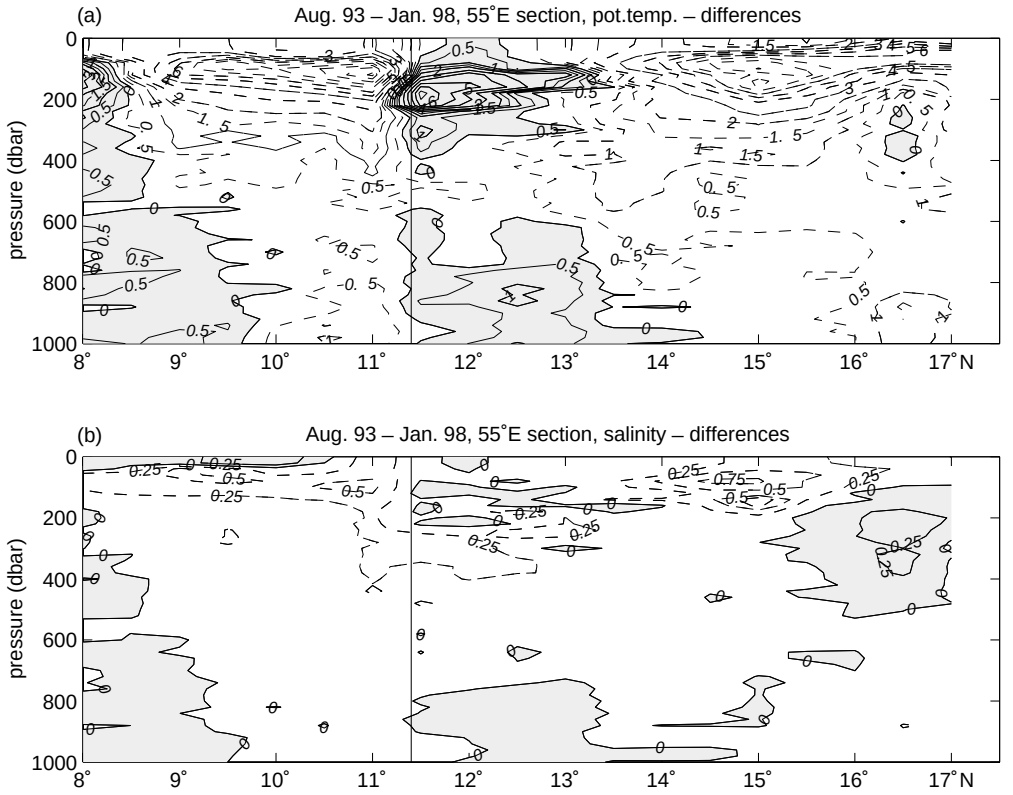

Fig. 7. Differences in (a) temperature with a contour interval of 0.5°C for differences of less than 2°C, else the contour interval is 1.0°C and (b) salinity for August 1993 compared to January 1998 (positive differences represent higher values in August 1993) for the northwestward section from 8°N to the Socotra Passage and then northward to the Arabian peninsula at about 56°30′E (see Fig. 1) with a zonal jump at 11°24′N (marked by a line), named here the 55°E section.

4.3.1. Ekman heat fluxes

First, the Ekman component of the heat transport was computed. The ERS wind data are available with weekly resolution and on a spatial grid of about 100×100 km. Following the ship's track, the wind data lying closest both in space and time were extracted from the ERS data matrix. The potential temperature for the heat computation was derived as a weighted average of temperature at the surface and at 50 m (Hall and Bryden, 1982). For the Ekman temperature we used 2 times the surface temperature plus the 50 m depth temperature divided by 3. The mixed layer along 8°N is at most locations 50 m or deeper (Fig. 9), hence using the upper 50 m as Ekman layer is a reasonable approximation. Other methods exist to define the depth of wind mixing like defining a top of the pycnocline (Chereskin et al., 2002); however, there appear also weaknesses with other methods as discussed by Chereskin et al. (2002). For example, in September 1995 the top of the pycnocline in the Great Whirl region in Chereskin et al.'s (2002) investigation was located below a layer with a temperature gradient of up to 14°C. Hence, we prefer to keep the simple approximation of 50 m depth for the Ekman layer depth. The small region of a shallow mixed layer in August 1993 near India is a region with relatively low winds and the error caused by using 50 m will be small. The Ekman-component of the heat flux across the sections was computed from the combination of the ERS scatterometer winds and the CTD data, yielding 0.89 PW in January 1998 and −0.84 PW in August 1993 (Table 2).

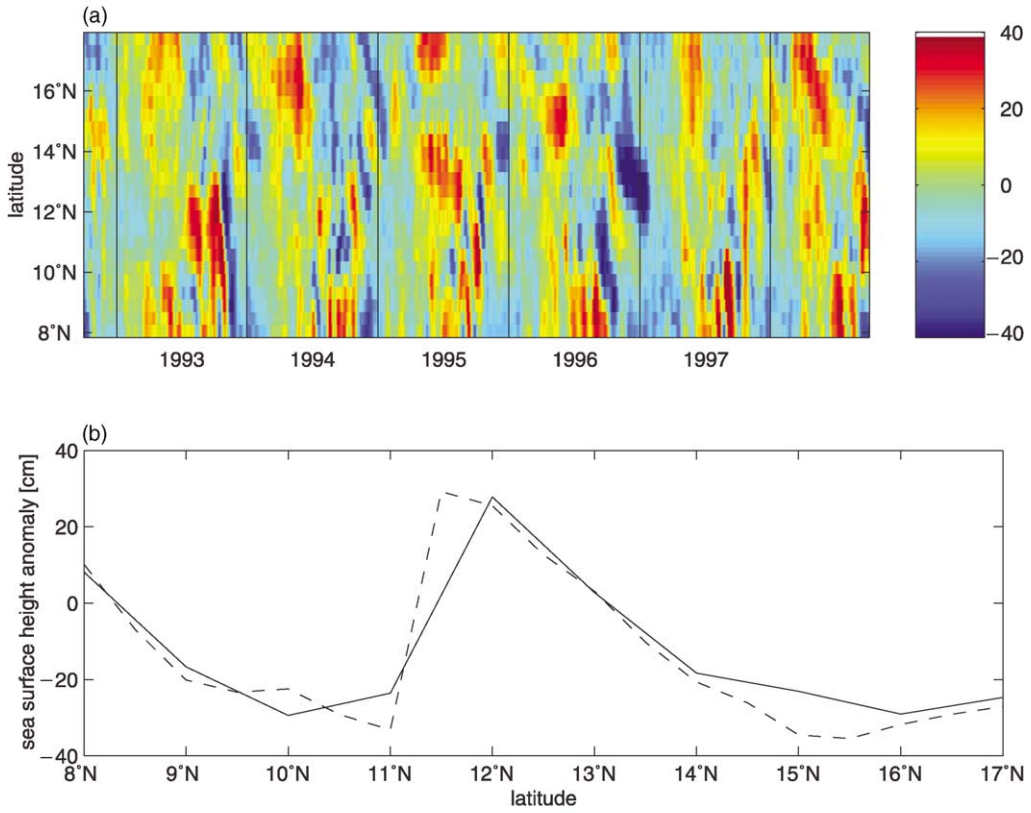

Fig. 8. (a) TOPEX/Poseidon sea surface height anomaly along path 233 (see Fig. 1) running from about 8°N, 55°E to 17°N, 58°E, is shown by latitude and time (top), (b) comparison of differences of sea surface height anomalies interpolated to the actual cruise track (solid line) and of integrated 0–1000 m density anomalies (dashed line) between August 1993 and January 1998 (bottom) along the 55°E section.

4.3.2. Heat fluxes west of Socotra

The section does not cover completely the exchanges through the Socotra Passage between the island of Socotra and the African continent (Fig. 1). For political reasons only the eastern part of the passage including the deep channel of the Socotra Passage was sampled, and for an estimate of the overall exchanges we have to extrapolate the data to the shallow part of the western shelf. On both cruises the westernmost ADCP measurements showed a northward velocity of about 20 cm/s in the upper 100 m. Using the distance to the African continent of 50 km and 100 m depth leads to a northward transport of 1.0 Sv. Using this transport and the temperature profile at the westernmost CTD-station leads to an estimate of the heat flux through the Socotra Passage of 0.10 PW in January 1998 and 0.09 PW in August 1993.

4.3.3. Geostrophic heat fluxes

For geostrophic computations a reference depth has to be determined. In the Atlantic Ocean, the boundaries between water masses spreading into different directions can be used as levels of slow motion. In the Arabian Sea the deeper water masses are moving slowly but with seasonal current fluctuations superimposed (e.g. Beal et al., 2000b). The water masses are difficult to separate, and hence the water mass distribution is of little help for the choice of the reference depth. For August 1993 Stramma et al. (1996) compared

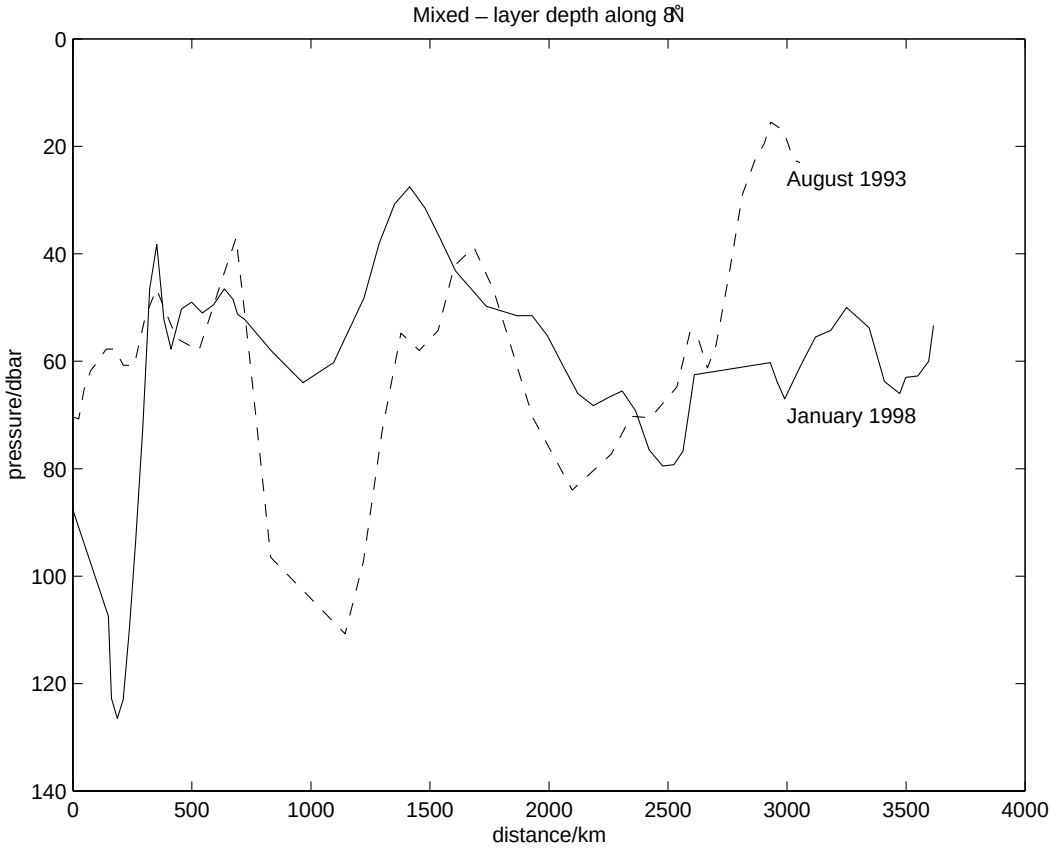

Fig. 9. Depth of the mixed layer defined as the depth of a temperature decrease of 0.5°C compared to the temperature at 5 m and smoothed by a weighted running mean over 3 points for August 1993 (dashed) and January 1998 (solid) from the Socotra Passage to 8°N and to the Indian shelf in 1993 and the Sri Lankan shelf in 1998. The 8°N section starts at 570 km, the Maldives are located near 2800 km.

geostrophic estimates with shipboard and lowered ADCP measurements for the eastern side of the 8°N section between 68°E and the Indian shelf. A 1000-m reference depth, which was successfully used in other analyses (Shetye et al., 1990), appears to be a reasonable choice. On the western side, in the Great Whirl region, with intense currents dominating the upper 300 m, a shallower reference near 400 m depth appears to be a reasonable reference for the investigation of the Great Whirl (Fischer et al., 1996). Observations in the same region during 1995 (Schott et al., 1997) showed, however, that currents exceeding 10 cm/s are present below the Great Whirl extending down to 1000 m depth and deeper. For January 1998 the direct current observations along the 53°E section off Somalia show at about 8.5–9°N a current band with about 10 cm/s reaching to almost 1000 m (Schott and Fischer, 2000; their Fig. 10), indicating that a reference of 1500 m seems to be the best choice.

As the transport between a station pair often shows large changes dependent on the reference depth, a variable reference depth along a section in general leads to a total transport that is strongly related to the exact location of changes in the reference depth. For an estimate of the total cross-section transports we therefore used a constant reference depth. This reference depth was varied (Fig. 10) until the residual transport across the

Table 2
Heat transport components for the African shelf between Africa and the Socotra Passage, for the Ekman transport computed from ERS weekly satellite derived wind data for January 1998 of 7.7 Sv and its error of ±3.0 Sv and for August 1993 of −7.4 Sv and its error of ±2.3 Sv and for the geostrophic transports relative to a fixed reference level to balance the African shelf and Ekman transports. In case of August 1993 three different reference layers balance each requested transport values

Month	ERS wind Ekman		African shelf		Geostrophic			Total heat (PW)
	Tr (Sv)	Heat (PW)	Tr (Sv)	Heat (PW)	Ref. level (dbar)	Tr (Sv)	Heat (PW)	
January 1998	7.7	0.89	1.0	0.10	1850	−8.7	−0.75	+0.24
January 1998	4.7	0.55	1.0	0.10	1970	−5.7	−0.66	−0.01
January 1998	10.7	1.24	1.0	0.10	1760	−11.7	−0.83	+0.51
August 1993	−7.4	−0.84	1.0	0.09	1210	6.4	0.19	−0.56
August 1993	−7.4	−0.84	1.0	0.09	920	6.4	0.47	−0.28
August 1993	−7.4	−0.84	1.0	0.09	2630	6.4	0.13	−0.62
August 1993	−9.7	−1.10	1.0	0.09	1260	8.7	0.21	−0.80
August 1993	−9.7	−1.10	1.0	0.09	800	8.7	0.53	−0.48
August 1993	−9.7	−1.10	1.0	0.09	2550	8.7	0.17	−0.84
August 1993	−5.1	−0.59	1.0	0.09	1140	4.1	0.20	−0.30
August 1993	−5.1	−0.59	1.0	0.09	1020	4.1	0.31	−0.19
August 1993	−5.1	−0.59	1.0	0.09	2710	4.1	0.09	−0.41

whole section matched the near-surface Ekman transport (Fiadeiro and Veronis, 1982). The bottom triangles were filled by constant extrapolation of the deepest geostrophic velocity computed.

The water loss through evaporation in the northern Arabian Sea is small compared to the ocean transports. The estimate of the freshwater loss of 125 mm/month given as winter value by Prasanna Kumar and Prasad (1999) leads to a loss of 0.1 Sv in the Arabian Sea north of 10°N. As there are no other large water sinks or sources in the Arabian Sea, the geostrophic transport has to balance the Ekman transport combined with the transport through the Socotra Passage. Using the scatterometer-derived Ekman transports (Table 1) and the estimated 1 Sv for the leakage in the Socotra Passage, a net geostrophic transport of −8.7 Sv in January 1998 and 6.4 Sv in August 1993 is required to balance the Ekman and Socotra-Passage contributions. In January 1998 there is only one reference level at 1850 dbar but in August 1993 there are 3 reference levels at 920, 1210 and 2630 dbar that give the corresponding net geostrophic transport (Fig. 10).

4.3.4. Total heat fluxes

The geostrophic heat flux components for the different solutions are −0.75 PW in January 1998 for the reference level of 1850 dbar. In August 1993 we estimate the geostrophic contribution at 0.47 PW for a reference at 920 dbar, 0.19 PW for a reference at 1210 dbar and 0.13 PW for a reference at 2630 dbar (Table 2). Combined with the contributions from the Ekman transport and Socotra Passage leakage, the net heat transport for the Arabian Sea across 8°N is 0.24 PW in January 1998 and it is −0.28 PW in August 1993 with a geostrophic reference of 920 dbar, −0.56 PW with a geostrophic reference of 1210 dbar and −0.62 PW with a geostrophic reference of 2630 dbar (Table 2).

The two realistic solutions with geostrophic references at 1210 and 2630 dbar for August 1993 result in −0.56 and −0.62 PW (hence a mean heat flux of about −0.6 PW) and the 0.24 PW for January 1998 are similar to the heat flux estimates derived from models and climatological data as shown by Garternicht and Schott (1997). According to Garternicht and Schott (1997, their Fig. 4) the heat fluxes estimated from the model and from climatological data are between 0.3 and 0.6 PW in January, and −0.4 to −0.8 PW in August at 8°N. The lower values observed here compared to the model results are not unreasonable, as in the observation only the overturning and fluxes in the Arabian Sea were taken into account, while the

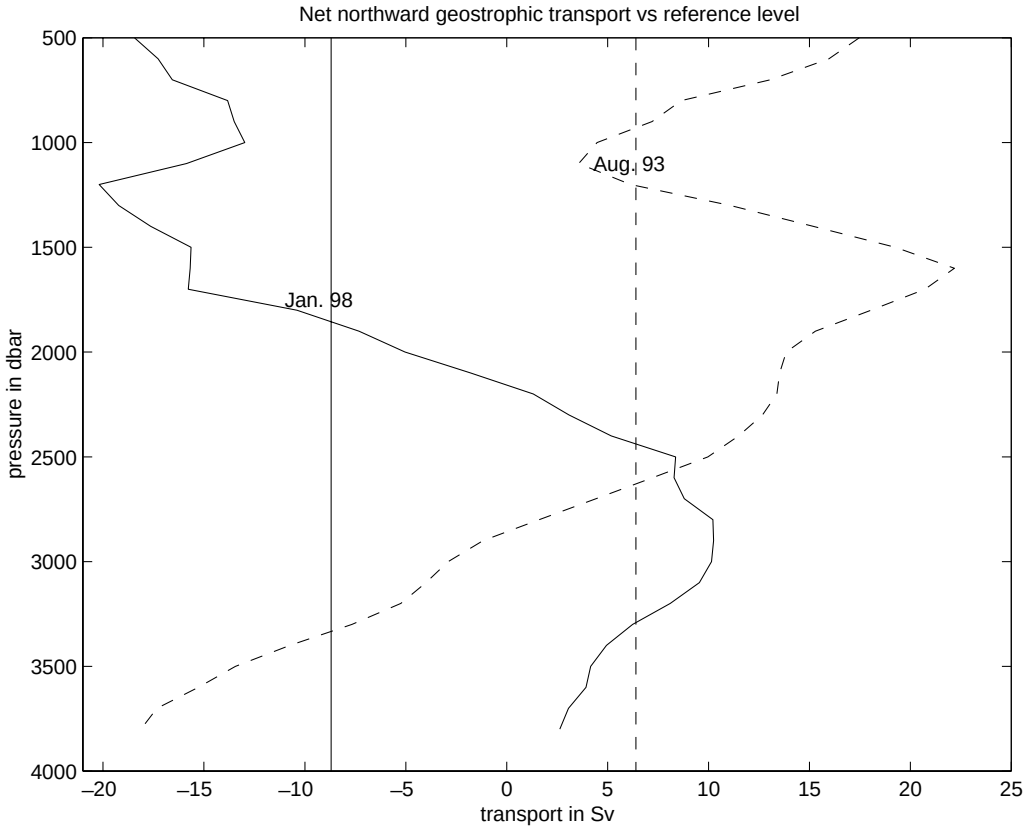

Fig. 10. Net geostrophic transport (positive northward) versus a moving reference depth for January 1998 (solid) and August 1993 (dashed line). The vertical lines show the required values of −8.7 Sv in January 1998 (solid line) and 6.4 Sv in August 1993 (broken line) that balance the Ekman transports.

model and climatological estimates also include contributions from the Bay of Bengal. For comparison a direct estimate exists from an 8°N-section across the Arabian Sea in September 1995. From the hydrographic observations Shi et al. (2002) estimated a heat transport of −0.60 PW, which agrees with our August 1993 estimate.

4.3.5. Freshwater fluxes

An estimate of the freshwater flux was performed for both R.V. *SONNE* cruises, and we assume that there were no long-term changes in the mean salinity along the 8°N section. The freshwater fluxes were computed following the method of Wijffels (2001). The differences of the observed salinity to the mean section salinity were integrated for the geostrophic velocity field, the Ekman velocity field and the leakage at the Socotra Passage, and the result was divided by the mean salinity. The mean salinity of a section was derived from the measured salinity that was first interpolated to an equally spaced grid. The mean salinities of 34.958 for August 1993, and 34.933 for January 1998 were significantly different. The difference was probably caused by both, somewhat different locations of the cruise tracks and seasonal changes of salinity in the upper ocean.

The freshwater flux computations across the 8°N section resulted in 0.43 Sv for August 1993 and 0.07 Sv for January 1998. When we use an annual mean salinity averaged over both cruises, instead of two individual mean salinities, the results differ only by about 1%. The positive

(northward) freshwater flux into the Arabian Sea in August and September is mainly caused by the strong southeastward Ekman flow of saline surface water. In January 1998 the Ekman flow is toward the northwest. However, on the eastern side of the Arabian Sea salinity-poor water from the Bay of Bengal is transported into the Arabian Sea, which again leads to a northward freshwater flux. Shi et al. (2002) described a comparable freshwater flux of 0.38 Sv for the Arabian Sea at 8°N for September 1995. These numbers are in agreement with the positive mean evaporation minus precipitation balance over most of the Arabian Sea (Wijffels, 2001), which requires a compensating freshwater flux into the Arabian Sea. However, our rough estimate of the winter value based on the the charts of Prasanna Kumar and Prasad (1999) led to an Evaporation–Precipitation (E−P) loss of only 0.1 Sv in the Arabian Sea. Their seasonal maps of E−P (their Fig. 8) indicate that this value is a maximum and is probably lower in the other seasons, hence the summer freshwater fluxes computed here and by Shi et al. (2002) seem to be too large to be caused solely by the E−P component and a freshwater storage term should be included.

Typically, the assumption for the direct freshwater flux computation across a section is that we measure the steady-state portion of the velocity and the salinity field, but in the tropics, seasonal and interannual changes in flux distribution and sea surface salinity become large, hence large uncertainties can be expected for the section across the Arabian Sea at 8°N. Wijffels (2001) states that uncertainties in the tropics may reach 0.3 Sv. To evaluate the seasonal changes we used the Levitus and Boyer (1994b, in the following called Levitus) $1^\circ \times 1^\circ$ salinity distribution based on full ocean depth and seasonally resolved profiles. The Levitus salinity values of the Arabian Sea north of 7.5°N were weighted by the thickness of the related depth intervals.

The total salt content for the Arabian Sea north of 7.5°N was 4.4148×10^{17} kg in winter (January–March), 4.7175×10^{17} kg in spring, 4.7166×10^{17} kg in summer and 4.7148×10^{17} kg in fall. To compensate the salt differences between the seasons a salt transport of about 0 in winter, of 3.47×10^{17} kg/s in spring, of -1.15×10^{17} kg/s in summer and -2.31×10^{17} kg/s in fall is necessary. The integration of the salt transport across our two sections resulted in a transport of -3.2×10^{17} kg/s in January 1998 and -8.2×10^{17} kg in August 1993. The August 1993 salt transport is even a little less than the required seasonal change from the Levitus data, hence the August 1993 salt or freshwater flux is mainly needed to compensate the seasonal change in salt content and only to a minor extent to compensate the E−P balance.

The computations for the sections were made to balance the volume flux components of geostrophic and Ekman flow and the Sokotra leakage. In case the 0.4 Sv northward freshwater flux is added, the results change only by a few percent. There are several uncertainties involved in the computations of the freshwater fluxes. Among these are uncertainties resulting from the interpolated Levitus salinity field, from the choice of geostrophic references, and from uncertainties in the wind fields and the corresponding Ekman transport. Further, the estimate of the E−P balance from seasonal maps and the freshwater flux equation applies only for a known long-term mean salinity. The results presented here, can therefore only be regarded as rough estimates of the fluxes. Nevertheless, it seems that the August 1993 freshwater flux was dominated by the change of the seasonal salinity storage rather than by the E−P balance, and we conclude that this component has to be taken into account for freshwater flux computations in regions of strong seasonal changes. The results derived from the Levitus seasonal salinity distribution show that in spring and fall the salt flux across 8°N in the Arabian Sea, owing to the seasonal salinity change, should be even larger than that derived for August 1993.

4.3.6. *Vertical overturning cell*

Fig. 11 shows the vertically upward integrated geostrophic section transport for the four reference layers. This transport combined with the Ekman transport and the Socotra Passage leakage of the upper 100 m results in negligible net transport across 8°N. In contrast, the 920 dbar reference (August 1993) led to an unrealistic

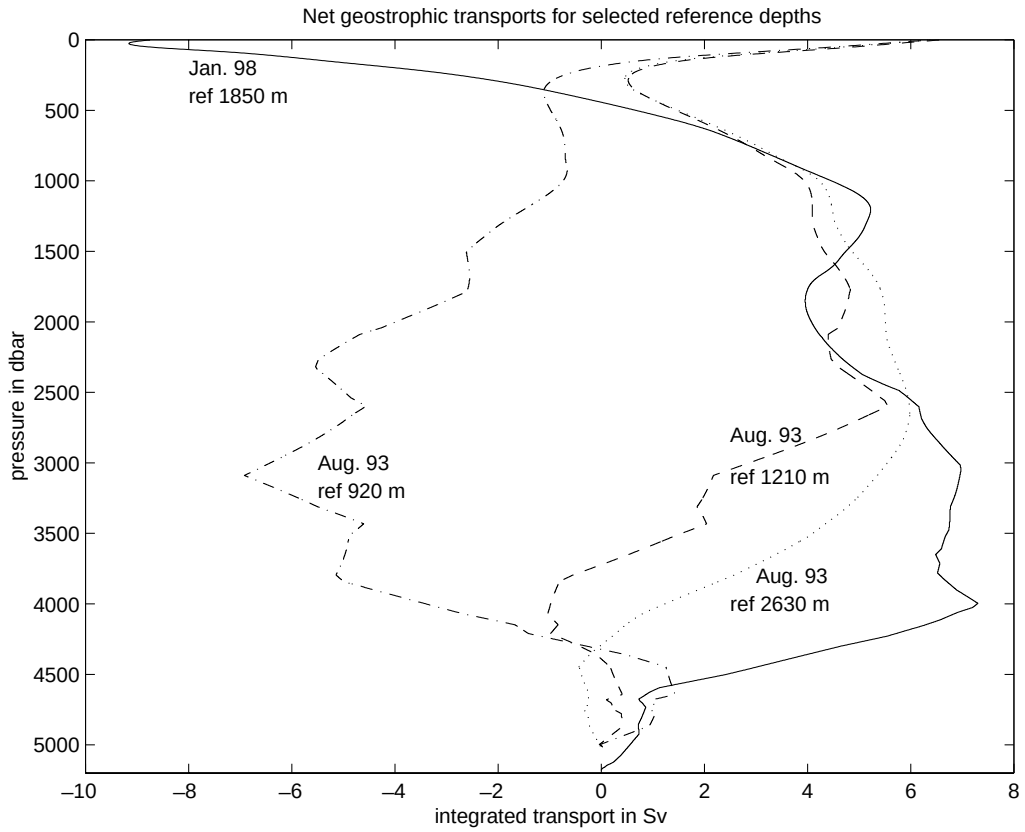

Fig. 11. Net geostrophic section transport (positive northward) integrated upward from the bottom with reference level at 1850 dbar for January 1998 (solid) and 920 dbar (dash-dotted), 1210 dbar (dashed) and 2630 dbar (dotted) for August 1993.

negative overturning circulation below 1000 m depth with southward flow near the bottom and northward flow at mid-depth. This is caused by strong velocity gradients near 900 m depth at the 55°E section, yielding large southwestward velocities in the deep ocean. All other solutions lead to a positive overturning circulation below 1000 m. According to these solutions there is a deep (below 2500 m depth) inflow of about 4–6 Sv into the deep Arabian Sea and an overlying outflow in the 300–2500 m layer. This deep overturning circulation is in agreement with the water mass distribution described above. Model computations (e.g. Wacongne and Pacanowski, 1996; Lee and Marotzke, 1997) do not show a deep vertical overturning circulation but limit the cell to the upper 1000 m. In contrast, Ganachaud et al. (2000) found a deep cell from a global hydrographic inverse box model. For three zonal sections in the South Indian Ocean they determined a deep inflow below 2000 dbar of 10.6 Sv at 32°S, and 10 Sv at 20°S and 8°S. As the overturning cell does not weaken in the subtropical South Indian Ocean, it appears reasonable that it continues into the northern hemisphere. A large fraction of the upwelling will take place in the Arabian Sea, where the strength of the overturning cell (at 8°N) was estimated to be between 4 and 6 Sv for both monsoon seasons. Using a different method to estimate the absolute geostrophic velocities Shi et al. (2002) estimated an upwelling of about 7 Sv from the deep Arabian Sea to the upper layers. Their upwelling estimate was based on data from the September 1995 section along 8°N and on a

slightly different method to derive absolute geostrophic velocities. Due to the choice of a constant reference depth and the method used for the extrapolation to the bottom there should be large uncertainties present in the computed strength of the overturning circulation. Thus, no attempt has been made to compute exact values for the overturning cell, but instead we would like to note that there are strong indications, that such an overturning cell exists.

The depth-integrated transport crosses 0 at 440 m in January 1998 and reaches almost 0 at 280 m depth in August 1993 for the two deep reference layers (Fig. 11), marking the boundary between the deep and shallow overturning cells. The small imbalance of 0.5 Sv near 300 m in August 1993 (Fig. 11) might be a small upwelling contribution to the upper ocean cell from the deep ocean cell. However, this value is small compared to all possible error influences. In the shallow cell the Ekman transport balances the geostrophic transport plus the 1 Sv leakage through the Socotra Passage. The cell changes direction between the monsoon seasons and is associated with upwelling in the northern basin during summer and downwelling during winter. This upwelling/downwelling is associated with an uplifting/depression of the stratification of the northern Arabian Sea. Hence, the water compensating the Ekman flow in the Indian Ocean near 8°N is restricted to the upper 300–450 m and the shallow cell thus only involves the near surface and upper intermediate water masses down to the Persian Gulf and Central waters. Red Sea Water and the North Indian Deep Water do not participate in the shallow cell overturning and are thus not ventilated to the surface.

5. Discussion

The described transport and heat flux changes across 8°N between January 1998 and August 1993 are influenced by changes in the water-mass distribution as well as by the annual Rossby waves that cover the entire width of the Arabian Sea (Brandt et al., 2002). In the western Arabian Sea the north–south section at about 55°E is mainly influenced by local processes except for the part south of 10°N, where the annual Rossby waves are still visible. A variational approach to balance the volume transports in the northern Arabian Sea resulted in reference levels for the geostrophic calculations of 1210 and 2630 dbar for August 1993 and of 1850 dbar for January 1998.

Direct current profile measurements made during the SO 89 cruise in August 1993 have been used to estimate transports related to regional current systems at the eastern and western section ends. Stramma et al. (1996) studied the current system off the Indian coast and found bands of alternating northward and southward currents. For the upper 300 m off India in August 1993 Stramma et al. (1996) estimated a geostrophic transport of 4.1 Sv based on a reference depth of 1000 m between the shelf and the flow reversal, between the reversal and 72°10′E of −4.7 Sv and between 72°10′E and 68°10′E of −2.9 Sv. The transports derived here for August 1993 with the reference of 1210 dbar lead to corresponding transports of 3.3, −5.1 and −2.3 Sv, respectively, which even better fit the transport derived from the lowered ADCP of 2.4, −6.2 and −2.4 Sv (Stramma et al., 1996). In their study of the Great Whirl based on the SO 89 observations, Fischer et al. (1996) used a shallow geostrophic reference at 400 dbar for closing box estimates of transports in areas with no direct current observations available. Recalculations of the transports with the reference (1210 dbar) used here led to similar results, with even small improvements in the transport balances.

The vertical overturning circulation and heat flux were computed for the northern Arabian Sea across the 8°N/55°E section. There are a number of uncertainties that make the results dependent on choices of the wind field for the estimate of the Ekman transport, the choice of the geostrophic reference, and the treatment of the bottom triangles. Nevertheless, there seems to be a clear indication of a deep vertical overturning circulation with water entering the deep Arabian Sea below 2500 m and leaving it in the depth range 300/450 m to 2500 m, in accordance with the water mass distribution. You (2000) computed dianeutral velocities for the Indian Ocean and reported

dianeutral upwelling for the deep water in the Arabian Sea. Between the surface and 300–450 m the compensating geostrophic and Ekman transports form a second shallow overturning cell. This cell is not stationary but changes its direction between summer and winter.

The heat fluxes across the section determined in this study were −0.60 PW in August 1993 and 0.24 PW in January 1998, and are in the range of earlier heat flux computations from models and climatologies (Garternicht and Schott, 1997). As the heat flux in the northern Arabian Sea is dominated by the Ekman flow, the results strongly depend on the choice of the wind field used. To estimate the errors in the heat fluxes caused by an errors in the wind field the estimated ERS-wind errors were added or subtracted to the wind data. The resulting Ekman heat fluxes range from 0.55 to 1.24 PW in January 1998 and from −0.59 to −1.10 PW in August 1993. The total heat flux from the combination of Ekman transport balanced by geostrophic transport leads to a heat flux range of 0.51 to −0.01 PW for January 1998 and from −0.19 to −0.84 PW for all 3 possible geostrophic reference levels in August 1993 (Table 2).

The total meridional heat flux across the 8°N section is dominated by the Ekman component, and its calculation correspondingly depends on good wind estimates. However, the geostrophic transports for January 1998 also were found to contribute significantly to the heat flux, because both, the near-surface layer and the upper branch of the deep overturning cell transport water southward (Fig. 11). By contrast, in August 1993 the geostrophic transports in the near-surface layer and in the upper branch of the overturning circulation were opposite to each other. Hence, the geostrophic contribution to the heat flux in the Arabian Sea is larger during the winter monsoon period than during the summer monsoon.

Freshwater flux computations across the two 8°N sections also were carried out and resulted in northward freshwater flux for both monsoon seasons. A comparison was made with climatological salinity fields (Levitus and Boyer, 1994b). We might expect some uncertainties in the Levitus salinity field caused by the interpolation scheme used. However, the surface to bottom difference in salinity computed from Levitus along 7.5°N between winter (34.919) and summer (34.941) of 0.022 is similar to the difference of 0.025 computed for our two sections at about 8°N. The evaluation of the salinity climatology showed that the larger freshwater flux in August 1993 can be explained by seasonal changes of the salinity storage in the Arabian Sea north of the 8°N section.

From ship drift observations (Cutler and Swallow, 1984; Shenoi et al., 1999) a cyclonic circulation is expected for January and anticyclonic flow for August. The upper ocean overturning cell appears to be confined to the upper 300–450 m. Therefore, the geostrophic transport for the upper 300 m was combined with the Ekman transport derived from the ERS1/2 wind data set and integrated eastward from the Socotra Passage to investigate how well the cyclonic and anticyclonic flow is developed (Fig. 12). There is no strong evidence of either cyclonic (winter monsoon) or anticyclonic (summer monsoon) flow, but weak indications of it. In January 1998 there is a weak southward component on the western side of the Arabian Sea, which is the Somali Current as described by Schott and Fischer (2000). Northward flow is found in the central and eastern part of the Arabian Sea, but west of the Maldives. This is partly compensated by strong southward flow east of the Maldives. Hence, we observed large-scale cyclonic flow in the central Arabian Sea (January 1998) and anticyclonic flow around the Maldives that is associated with the Laccadive High.

In August 1993 the northward transport is observed in the Great Whirl (the left peak in Fig. 12a) but a large amount of the Great Whirl returns southward and a second northward band east of the Great Whirl as described by Fischer et al. (1996) carries water into the Arabian Sea from lower latitudes. This water returns southward in broad flow in the central and eastern Arabian Sea; hence the anticyclonic flow in August 1993 is restricted to the region east of the Great Whirl.

Rossby waves with annual periods play an important role in the seasonally reversing baroclinic currents and transports of the central Arabian Sea (Brandt et al., 2002). Cumulative

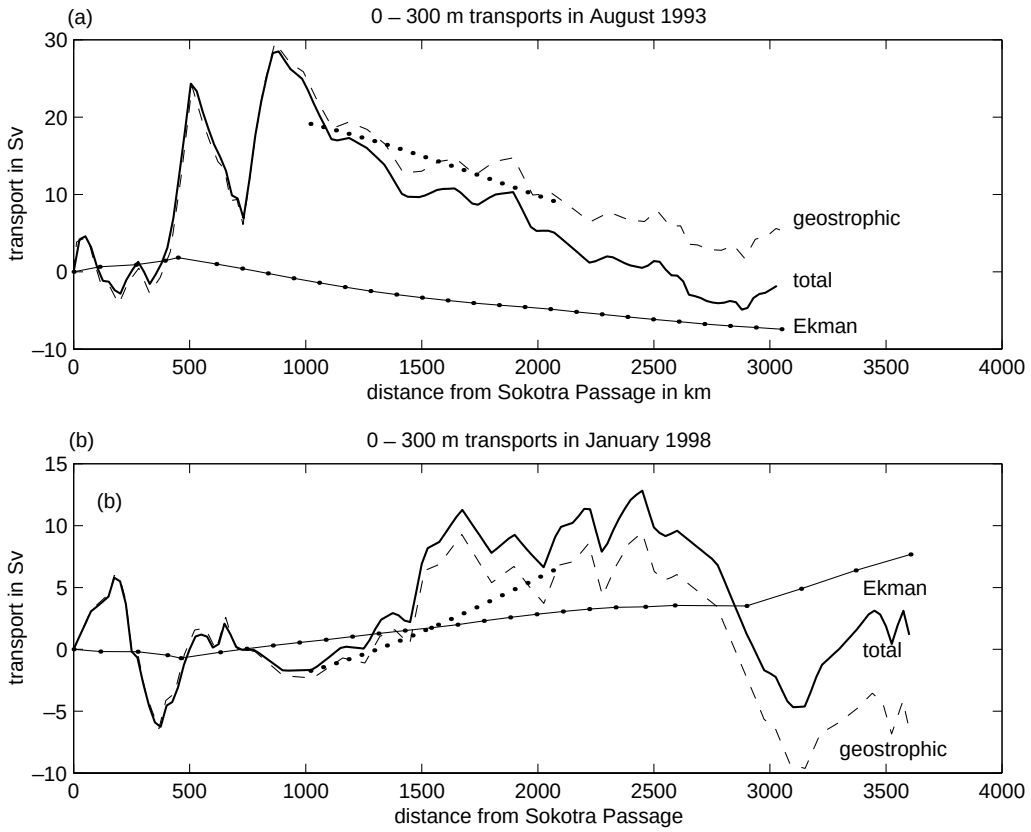

Fig. 12. Geostrophic transport (dashed), Ekman transport from the ERS1/2 winds (line with solid dots), total (solid) transport in the upper 300 m integrated from the Socotra Passage eastward and cumulative Rossby wave transport for the upper 300 m from 58°E to 68°E (dots, curve shifted to fit the geostrophic curve at 68°E; from Brandt et al., 2002) for (a) August 1993 with geostrophic reference 1210 dbar to the Indian shelf and for (b) January 1998 with geostrophic reference 1850 dbar to the Sri Lankan shelf. The 8°N section starts at 570 km, the Maldives are located near 2800 km.

transports for the near-surface layer (upper 300 m) have been presented for both cruises and the region between 58°E and 68°E; these are included in Fig. 12 for comparison with the Rossby wave transports of Brandt et al. (2002). Their transport in August 1993 was 9.8 Sv southward and in January 1998 8.0 Sv northward (their Fig. 10). The geostrophic 0–300 m transport derived here for 58–68°E is −13.9 Sv in August 1993 and 9.1 Sv in January 1998. Although the geostrophic transports are a little larger than the Rossby wave transports (Fig. 12), the geostrophic transports are clearly dominated by the annual Rossby waves in the central Arabian Sea.

The two cruises were carried out at phases of anomalous wind conditions during Indian Ocean 'dipole mode' episodes (Webster et al., 1999; Schott and McCreary, 2001). In August 1993 the winds near India and Sri Lanka were lower than normal and in early 1998 the Indian Ocean was influenced by the Indian Ocean warming with the appearance of a dipole mode in the tropical region and persistent basin-scale warming (Yu and Rienecker, 2000). Although these anomalous conditions influenced the local water mass distribution and currents near India in August 1993 and the mixed-layer temperature in January 1998, their influence on the basin-wide comparison of the Arabian Sea near 8°N seems to be limited. The meridional Ekman transport differences compared to the mean at the time of the cruise were <1 Sv.

Acknowledgements

We thank the captains and crew members of the R.V. *SONNE* for their help during the cruises. We acknowledge financial support by the Bundesministerium für Bildung und Forschung, Bonn, Germany, grants 03F157A, 03F0246A, 03R430, 03G0127A and 03G0128A as part of the German WOCE and CLIVAR programs. We also thank T. Chereskin for helpful comments.

References

Beal, L.M., Ffield, A., Gordon, A.L., 2000a. Spreading of Red Sea overflow waters in the Indian Ocean. Journal of Geophysical Research 105, 8549–8564.

Beal, L.M., Molinari, R.L., Chereskin, T.K., Robbins, P.E., 2000b. Reversing bottom circulation in the Somali Basin. Geophysical Research Letters 27, 2565–2568.

Brandt, P., Stramma, L., Schott, F., Fischer, J., Dengler, M., Quadfasel, D., 2002. Annual Rossby waves in the Arabian Sea from TOPEX/POSEIDON altimeter and in situ data. Deep-Sea Research II 49, 1197–1210.

Bruce, J.G., Johnson, D.R., Kindle, J.C., 1994. Evidence for eddy formation in the eastern Arabian Sea during the northeast monsoon. Journal of Geophysical Research 99, 7651–7664.

Chereskin, T.K., Wilson, W.D., Bryden, H.L., Ffield, A., Morrison, J., 1997. Observations of the Ekman balance at 8°30′N in the Arabian Sea during the 1995 southwest monsoon. Geophysical Research Letters 24, 2541–2544.

Chereskin, T.K., Wilson, W.D., Beal, L.M., 2002. The Ekman temperature and salt fluxes at 8°30′N in the Arabian Sea during the 1995 southwest monsoon. Deep-Sea Research II 49, 1211–1230.

Cutler, A.N., Swallow, J.C., 1984. Surface currents of the Indian Ocean (to 25°S, 100°E): compiled from historical data archived by the Meteorological Office, Bracknell, UK Institute of Oceanographic Sciences, Report no. 187, 8pp and 36 charts.

Dengler, M., 2000. Über die Tiefenzirkulation und die vertikale Vermischung im nordwestlichen Indischen Ozean. Ph.D. Thesis, University of Hamburg, 200pp.

Fiadeiro, M.E., Veronis, G., 1982. On the determination of absolute velocities in the ocean. Journal of Marine Research Supplement to Volume 40, 159–192.

Fischer, J., Schott, F., Stramma, L., 1996. Currents and transports of the Great Whirl-Socotra Gyre system during the summer monsoon, August 1993. Journal of Geophysical Research 101, 3573–3587.

Fu, L., Christensen, E.J., Yamarone, C.A., Lefebvre, M., Menard, Y., Dorrer, M., Escudier, P., 1994. TOPEX/POSEIDON mission overview. Journal of Geophysical Research 99, 24369–24381.

Ganachaud, A., Wunsch, C., Marotzke, J., Toole, J., 2000. Meridional overturning and large-scale circulation of the Indian Ocean. Journal of Geophysical Research 105, 26117–26134.

Garternicht, U., Schott, F., 1997. Heat fluxes of the Indian Ocean from a global eddy-resolving model. Journal of Geophysical Research 102, 21147–21159.

Gordon, A.L., 1986. Interocean exchange of thermocline water. Journal Geophysical Research 91, 5037–5046.

Hall, M.M., Bryden, H.L., 1982. Direct estimates and mechanisms of ocean heat transport. Deep-Sea Research A 29, 339–359.

Hellerman, S., Rosenstein, M., 1983. Normal monthly wind stress over the world oceans with error estimates. Journal of Physical Oceanography 13, 1093–1104.

Johnson, G.C., Warren, B.A., Olson, D., 1991a. Flow of bottom water in the Somali Basin. Deep-Sea Research I 38, 637–652.

Johnson, G.C., Warren, B.A., Olson, D., 1991b. A deep boundary current in the Arabian Sea. Deep-Sea Research I 38, 653–661.

Lee, T., Marotzke, J., 1997. Inferring meridional mass and heat transports of the Indian Ocean by fitting a general circulation model to climatological data. Journal of Geophysical Research 102, 10585–10602.

Le Provost, C., Lyard, F., Molines, J.M., Genco, M.L., Rabilloud, F., 1998. A hydrodynamic ocean tide model improved by assimilating a satellite altimeter-derived data set. Journal of Geophysical Research 103, 5513–5530.

Levitus, S., Boyer, T., 1994a. World Ocean Atlas 1994, Vol. 4: Temperature. NOAA Atlas NESDIS 4, US Government Printing Office, Washington DC, 117pp.

Levitus, S., Boyer, T., 1994b. World Ocean Atlas 1994, Vol. 3: Salinity. NOAA Atlas NESDIS 3, US Government Printing Office, Washington DC, 93pp.

Mantyla, A.W., Reid, J.L., 1995. On the origins of deep and bottom waters of the Indian Ocean. Journal of Geophysical Research 100, 2417–2439.

Morrison, J.M., 1997. Inter-monsoonal changes in the T–S properties of the near-surface waters of the northern Arabian Sea. Geophysical Research Letters 24, 2553–2556.

Pond, S., Pickard, G.L., 1983. Introductory dynamic oceanography, 2nd Edition. Pergamon Press, Oxford, 329pp.

Prasanna Kumar, S., Prasad, T.G., 1999. Formation and spreading of Arabian Sea high-salinity water mass. Journal of Geophysical Research 104, 1455–1464.

Qiu, B., Huang, R.X., 1995. Ventilation of the North Atlantic and North Pacific: subduction versus obduction. Journal of Physical Oceanography 25, 2374–2390.

Quadfasel, D., Fischer, J., Schott, F., Stramma, L., 1997. Deep water exchange through the Owen Fracture Zone in the Arabian Sea. Geophysical Research Letters 24, 2805–2808.

Schott, F., Fischer, J., 2000. The winter monsoon circulation of the northern Arabian Sea and Somali Current. Journal Geophysical Research 105, 6359–6376.

Schott, F.A., McCreary., Jr, J.P., 2001. The monsoon circulation of the Indian Ocean. Progress in Oceanography 51, 1–123.

Schott, F., Reppin, J., Fischer, J., Quadfasel, D., 1994. Currents and transports of the Monsoon Current south of Sri Lanka. Journal of Geophysical Research 99, 25127–25141.

Schott, F., Fischer, J., Garternicht, U., Quadfasel, D., 1997. Summer monsoon response of the northern Somali Current, 1995. Geophysical Research Letters 24, 2565–2568.

Shankar, D., Shetye, S.R., 1997. On the dynamics of the Lakshadweep high and low in the southeastern Arabian Sea. Journal of Geophysical Research 102, 12551–12562.

Shenoi, S.S.C., Saji, P.K., Almeida, A.M., 1999. Near-surface circulation and kinetic energy in the tropical Indian Ocean derived from Lagrangian drifters. Journal of Marine Research 57, 885–907.

Shetye, S.R., Gouveia, A.D., Shenoi, S.S.C., Sundar, D., Michael, G.S., Almeida, A.M., Santanam, K., 1990. Hydrography and circulation of the west coast of India during the southwest monsoon 1987. Journal of Marine Research 48, 359–378.

Shetye, S.R., Gouveia, A.D., Shenoi, S.S.C., 1994. Circulation and water masses of the Arabian Sea. In: Lal, D. (Ed.), Biogeochemistry of the Arabian Sea. Indian Academy of Sciences, Bangalore, pp. 9–25.

Shi, W., Morrison, J.M., Bryden, H.L., 2002. Water, heat and freshwater flux out of the northern Indian Ocean in September–October 1995. Deep-Sea Research II, this issue.

Stramma, L., Fischer, J., Schott, F., 1996. The flow field off southwest India at 8N during the southwest monsoon of August 1993. Journal of Marine Research 54, 55–72.

Swallow, J.C., Fieux, M., 1982. Historical evidence for two gyres in the Somali Current. Journal of Marine Research 40, 747–755.

Swallow, J.C., Molinari, R.L., Bruce, J.G., Brown, O.W., Evans, R.H., 1983. Developments of near-surface flow pattern and water mass distribution in the Somali Basin in response to the southwest monsoon of 1979. Journal of Physical Oceanography 13, 1398–1415.

Swallow, J.C., Fieux, M., Schott, F., 1988. The boundary currents east and north of Madagascar, Part I: geostrophic currents and transports. Journal of Geophysical Research 93, 4951–4962.

Tomczak, M., Godfrey, J.S., 1994. Regional Oceanography: An introduction. Elsevier, Oxford, 422pp.

Wacongne, S., Pacanowski, R., 1996. Seasonal heat transport in a primitive equations model of the tropical Indian Ocean. Journal of Physical Oceanography 26, 2666–2699.

Warren, B., 1993. Circulation of north Indian deep water in the Arabian Sea. In: Desai, B.N. (Ed.), Oceanography of the Indian Ocean, Balkema, Rotterdam, pp. 575–582.

Warren, B.A., Johnson, G.C., 1992. Deep currents in the Arabian Sea in 1987. Marine Geology 104, 279–288.

Warren, B., Stommel, H., Swallow, J.C., 1966. Water masses and patterns of flow in the Somali Basin during the southwest monsoon of 1964. Deep-Sea Research 13, 825–860.

Webster, P.J, Moore, A.M., Loschnigg, J.P., Leben, R.R., 1999. Coupled ocean-atmosphere dynamics in the Indian Ocean during 1997–98. Nature 401, 356–360.

Wijffels, S.E., 2001. Ocean transport of fresh water. In: Siedler, G., Church, J., Gould, J. (Eds.), Ocean Circulation and Climate, Observing and Modelling the Global Ocean. Academic Press, London, pp. 475–488.

Wyrtki, K., 1973. Physical oceanography of the Indian Ocean. In: Zeitzschel, B., Gerlach, S.A. (Eds.), The Biology of the Indian Ocean. Chapman & Hall, London, pp. 18–36.

You, Y., 2000. Implications of the deep circulation and ventilation of the Indian Ocean on the renewal mechanism of North Atlantic deep water. Journal of Geophysical Research 105, 23895–23926.

Yu, L., Rienecker, M.M., 2000. Indian Ocean warming of 1997–1998. Journal of Geophysical Research 105, 16923–16939.